IEEE Access
Multidisciplinary | Rapid Review | Open Access Journal

Received February 27, 2020, accepted April 4, 2020, date of publication April 7, 2020, date of current version April 21, 2020.

Digital Object Identifier 10.1109/ACCESS.2020.2986393

Research on Novel Direct Instantaneous Torque Control Strategy for Switched Reluctance Motor

SHUANGHONG WANG, ZIHUI HU, AND XIUPENG CUI, (Member, IEEE)
State Key Laboratory of Advanced Electromagnetic Engineering and Technology, School of Electrical and Electronic Engineering, Huazhong University of Science and Technology, Wuhan 430070, China

Corresponding author: Zihui Hu (bella2hu@163.com)

ABSTRACT In order to solve the frequent problem of breaking shaft in the starter/generator system of switched reluctance motor, a novel Direct Instantaneous Torque Control (DITC) is proposed to control the torque ripple in this paper. Instead of the hysteresis controller in traditional DITC, the PWM is introduced to modulate the torque deviation; the optimal switching signal is selected according to the PWM modulation signal and the sector where the rotor position is located. Based on the torque characteristic curves, the torque ripple during commutation period is analyzed and the compensation methods are proposed. Simulation results prove that the compensated PWM-DITC can suppress the torque ripple of switched reluctance motor effectively.

INDEX TERMS Switched reluctance motor (SRM), direct instantaneous torque control, fixed switching frequency.

I. INTRODUCTION

As a new generation of drive motor, switched reluctance motor (SRM) has simple structure, no winding on the rotor side, high operating efficiency; unipolar current, few power devices, and high reliability; Each phase runs independently with high fault tolerance [1]–[4]. The bidirectional flow of energy without attachments makes switched reluctance motors particularly suitable for using in aerospace starting and generation systems [5]–[9]. However, SRM's special double-salient structure and high saturation nonlinear magnetic circuit make it have large torque ripple [10]–[12]. It would cause the transmission system shaft oscillation, even lead to break shaft causing engine damage [13]. Torque ripple seriously hinders the application of SRM in aerospace starting and generating systems. The research focusing on torque ripple suppression has great engineering value, and is an urgent problem to be solved at present.

Many scholars have conducted in-depth research on the torque ripple of SRM. From the perspective of motor design, it can be realized by motor optimization scheme [10], [14]–[16], such as rotor slant pole and air gap optimization. From the perspective of control strategy, direct torque control (DTC) [17]–[19] is derived from the AC motor control system. Based on flux linkage and torque double hysteresis loop, the flux magnitude and rotation speed of the flux linkage are controlled by selecting the appropriate voltage vector to achieve torque control. Combined with the flux characteristics of SRM, literatures [20]–[23] eliminates the redundant design of the flux linkage closed-loop, and proposes direct instantaneous torque control (DITC), The control algorithm is greatly simplified, but there is a switching frequency uncontrollable problem; To realize accurate distribution of the front-rear phase torque in the commutation interval, torque sharing function (TSF) [24]–[26] selects the appropriate distribution function based on mathematical modeling. Model predictive control (MPC) [27], [28] predicts the future state from the current state according to the state equation, sets the cost function and minimizes it to determine the optimal control signal. It depends on accurate motor modeling, and the more objects the cost function expects to control, the larger the amount of calculation. Neural network control (NNC) [29], [30] requires enough data training models to realize autonomous control, which takes a long time in the early stage. Because of the complexity of the algorithm, intelligent control is restricted in practical application.

In order to solve the problem that switching frequency of DITC is out of control, this paper proposes a novel DITC control strategy. Compared with the traditional DITC, the torque hysteresis is removed and the PWM control is used to fix

The associate editor coordinating the review of this manuscript and approving it for publication was M. Venkateshkumar.

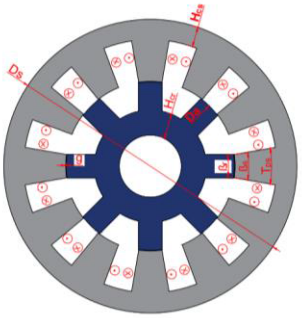

FIGURE 1. Three-phase 12/8-pole SRM cross-section.

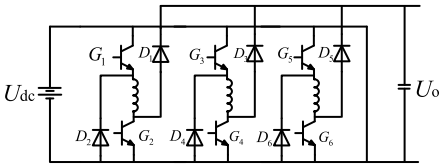

FIGURE 2. Three-phase asymmetric half-bridge circuit.

the switching frequency. The commutation interval is further divided according to characteristic curves among torque, position and current. By adjusting coefficients of duty cycle in different sectors, the torque ripples can be suppressed effectively and the current can be controlled reasonably to improve the motor efficiency at the time.

II. NON-LINEAR MODEL OF SRM

SRM realizes the correlation transformation of electrical energy and mechanical energy through reluctance torque. Considering SRM starting/generating system taking into account both torque ripple under electric state and efficiency under power generation state, three-phase 12/8 pole SRM is selected as the research object of this paper. Figure 1 is the three-phase 12/8 pole SRM section diagram. Each phase winding contains four sets of coils, which can be connected in series or parallel according to requirements. Figure 2 shows the most widely used three-phase asymmetric half-bridge circuit in SRM, which can realize independent control of three-phase winding. There is no bridge arm straight-through phenomenon, thus the control is simple and reliable. According to the on-off state of the upper and lower tubes, each phase winding has three working modes: excitation mode, freewheel mode and demagnetization mode. Demagnetization mode can supply electric energy to the outside world in the state of power generation. Taking A-phase winding in the electric state as an example, when the upper and lower switching tubes G_1, G_2 are both switched on, the winding is subjected to a positive voltage, and the winding current rises, which is called the excitation mode. When one of the two tubes is switched on and the other is switched off, such as G_2 is switched on and G_1 is switched off, and the winding current passes through the switch tube G_2 and freewheeling diode D_2 to form a channel, voltage on the winding is near zero, and the winding current drops slowly, which is called the

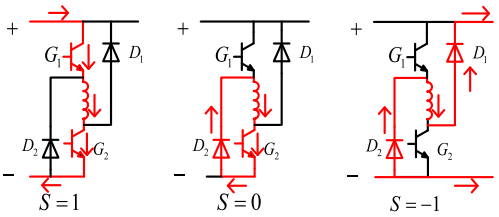

FIGURE 3. Three modes of operation of the phase winding.

freewheeling mode. When switch tubes G_1 and G_2 are both turned off, the winding is subjected to negative voltage, the phase current passes through the freewheeling diode D_1, D_2 and the energy feedback, the winding current drops rapidly, which is called demagnetization mode, the three working modes are shown in Figure 3. For convenience of explanation, $S = 1$ is the excitation mode, $S = 0$ is the freewheeling mode, and $S = -1$ is the demagnetization mode.

Considering the voltage drop on the switching tubes and diodes, the phase voltage U_k can be expressed as:

$$U_k = \begin{cases} U_{dc} - 2U_T & S = 1 \\ -(U_D + U_T) & S = 0 \\ -(U_{dc} + 2U_D) & S = -1 \end{cases} \tag{1}$$

where, U_T and U_D are respectively the voltage drop on the switch tubes and diodes, U_{dc} is the excitation voltage.

Ignoring the mutual inductance between windings, the voltage equation, flux equation and motion equation in SRM model are expressed as followsAF

$$\begin{cases} V_k = Ri_k + \frac{d\psi_k}{dt} \\ \psi_k = \psi_k(i_k, \theta) \\ J\frac{d\omega}{dt} = T_e - T_L - \alpha\omega \\ \omega = \frac{d\theta}{dt} \end{cases} \tag{2}$$

where, V_k, i_k, ψ_k, R are the voltage, current, flux and resistance on the k-phase winding respectively; T_e, $T_L$are total electromagnetic torque and externally applied load torque respectively; J, α, ω, θ are respectively the moment of inertia, wind-friction coefficient, motor speed and rotor position Angle.

The electromagnetic torque T_k generated by each phase winding is expressed asAF

$$T_k = \frac{\partial W_c(\theta, i_k)}{\partial \theta}|_{i_k=\text{const}} \tag{3}$$

where $W_c = \int_0^i \psi(\theta, i)di$ is co-energy.

The SRM model is highly nonlinear because of the special double-salient pole structure and the saturated working state. The data calculated by the simple linear model is far from the actual value, so the reference value of the simulation is poor, and complex models increase the computational burden. In this paper, the magnetic flux characteristics Ψ-i-θ and Torque characteristics T_e-i-θ are obtained by finite element calculation based on the designed SRM structure parameters, as shown in figure 4. The current curve i-Ψ-θ is obtained by

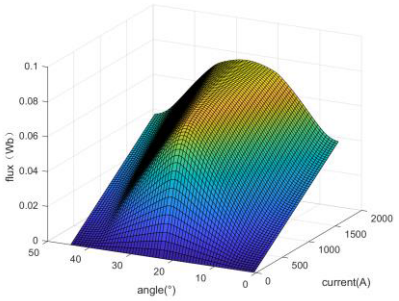

FIGURE 4. Magnetic flux characteristic surface.

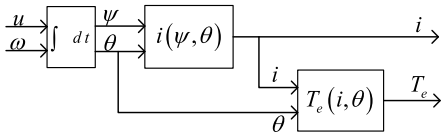

FIGURE 5. SRM nonlinear modeling structure.

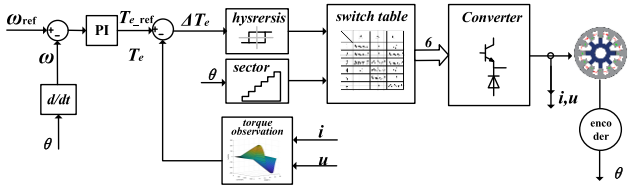

FIGURE 6. Traditional DITC control system block diagram.

two - dimensional interpolation inversion of flux characteristics, then adoption of the lookup-table method to build the motor nonlinear model, as shown in figure 5, which can truly and accurately reflect the electromagnetic characteristics of the SRM in the actual working state to the maximum extent.

III. TRADITIONAL DITC

Traditional DITC principle block diagram of the control system is shown in figure 6, DITC takes the synthesize instantaneous output torque as the direct control object, and inputs the difference between the given torque and the estimated torque to hysteresis controller. Combined with sector and hysteresis output, the appropriate switch signal is determined according to the switching table, so as to realize the control of synthesis torque. The given torque is acquired by PI controller of the outer loop. In the starter-generator system, speed is the control object of outer loop in electric state, while voltage is the control object of outer loop in generation state. As long as the sector is reasonably allocated, DITC can switch freely in the state of electric and generation.

IV. THE PROPOSED DITC

Since the SRMs work in the high saturation nonlinear state, at different positions and within different currents, the torque varies with the same voltage applied. In the ideal DITC, in order to control the torque ripple within a certain range, the controller should be able to respond quickly and change the state of the switch tube when the torque deviation signal is greater than or equal to the hysteresis upper and lower limits. This means that locations where torque changes dramatically require higher switching frequency. The simulation results show that the maximum switching frequency can reach 500 kHz, which is far beyond the current experimental level. Processing performance of existing data processors (DSP) and the thermal effect of power devices limit the maximum switching frequency. In addition, considering the time required for algorithm execution in each control cycle, the switching frequency is set as 20 kHz. At a lower control frequency, DITC could not respond to the hysteresis limit in time. If positive voltage, zero voltage or negative voltage is applied in the whole control cycle, torque change will be greater than expected, leading to big torque ripples. Therefore, it is necessary to reasonably control the action time of positive voltage, zero voltage and negative voltage according to SRM torque characteristic curve.

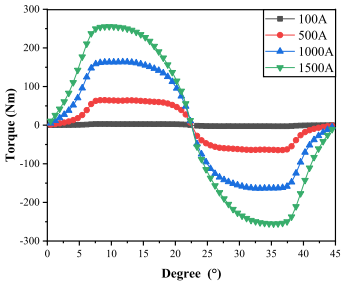

FIGURE 7. SRM torque characteristic curve.

A. TORQUE CHARACTERISTIC ANALYSIS

In the traditional DITC, it is divided into 6 sectors according to the three-phase conduction state, and different hysteresis control strategies are adopted for the single-phase and commutation interval, but torque characteristics have not been considered fully. In order to control the torque reasonably, taking the torque characteristics of 12/8 motor as example, the relationship between electromagnetic torque and rotor position under different current conditions is shown in figure 7. The x-coordinate is the rotor position in one mechanical period, and the starting position angle is the point when the stator salient pole is aligned with the axis of the rotor groove. The alignment of stator salient pole and rotor salient pole axis is 22.5°. Torque is symmetrical about midpoint position. At the same rotor position, torque is proportional to current. In the same current level, the torque variation trend is consistent with the inductance characteristic curve. It can be seen that when the rotor angle is between 0° and 4°, the inductance curve is relatively gentle, the current change rate is fast, but the torque value is small. At this point, the front-phase torque is still near the maximum value of the torque, so the main torque in this area is still provided by the front-phase. As the angle increases, bigger than 4°, the inductance increases rapidly, the current change rate slows down, and the torque starts to be established. At 15° ∼18°, the rising slope of the inductor decreases, and so does the torque. Moreover, the torque change rate under large current is faster than that under small current. As for the to-be switched off phase in the

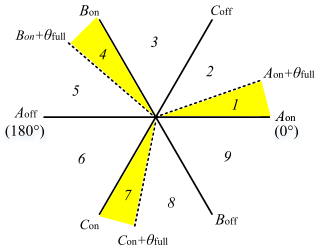

FIGURE 8. Schematic diagram of sector division.

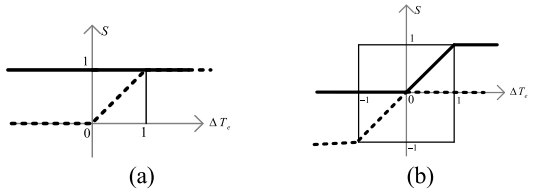

FIGURE 9. PWM control signal in the commutation interval. (a)Sector 1. (b) sector 2.

commutation interval, in order to maintain large torque all the time, higher current value is required. On one hand, it is easy to cause the extension of freewheeling time after switching off and generate negative torque. On the other hand, the larger the flow current value in the front-phase, the faster the torque decline rate will be when it turns off, and the difficulty of complementary torque in the rear phase will be increased. Therefore, the angle range which torque is mainly provided by front-phase at the commutation interval should be as small as possible. At 18° ∼22.5°, the inductance remains at the maximum value and the torque drops sharply. Considering that the current also drops rapidly when the phase winding is turned off, the actual torque decline rate is the superposition of the current change rate and the inductance change rate. Therefore, a new sector is added at the basis of the original commutation interval, as shown in figure 8. In the new sector, maintain the front-phase torque, establish the rear phase current at the same time, and take the new sector $\theta_{\text{full}} = 2°$.

B. CONTROL STRATEGY

Discrete sampling of torque deviation signals, compare it with unipolar carrier, and produce PWM control signal. Single-phase conducted interval outputs PWM signals with polarity 0 and 1, respectively representing zero voltage and positive voltage. The PWM control in the commutation interval is shown in figure 9. The x-coordinate is the torque error, and 1 is the upper limit amplitude of the carrier. The y-coordinate is the control signal, 1 represents the positive voltage, 0 represents the zero voltage, and -1 represents the negative voltage. In the figure, the solid line represents the after-phase and the dotted line represents the front-phase. Take sector 1, 2 as an example:

In sector 1, inductance of phase A is small, the current change rate is large, and the current can be quickly established, but the torque value is small; and phase C is still in the rising stage of inductance. So, in order to keep the electromagnetic torque constant, phase C provides the main torque. When the torque deviates ΔT_e is larger than the carrier, positive voltage is applied to phase C, and the current rises and the torque increases; When the torque deviates ΔT_e is smaller than the carrier, zero voltage is applied to phase C, keeping freewheeling to reduce the torque. Phase A maintains the positive voltage conducted all times, rapidly establishing the current and preparing for the rapid establishment of the subsequent torque.

In sector 2, with the inductance of phase A gradually increasing, A-phase torque rapidly increases since A-phase current in the previous sector has been fully established. Phase C is near the maximum value of the inductance, the change rate of the inductance decreases, and the torque begins to decline. At this point, although the phase C can maintain the same torque, it needs a larger current value, which is easy to cause overcurrent. Therefore, when the torque deviates ΔT_e is greater than 0, zero voltage is applied to phase C; if ΔT_e is greater than the carrier, positive voltage is applied to phase A, and the total torque is increased mainly by phase A. If ΔT_e is less than 0, apply zero voltage to phase A; when $|\Delta T_e|$ is larger than the carrier, negative voltage is applied to the phase C, and the total torque is reduced by the phase C; when $|\Delta T_e|$ is smaller than the carrier, zero voltage is applied to the phase C.

C. DUTY CYCLE CONTROL

In PWM control, the duty cycle of output signal is positively correlated with the modulation ratio of input. If the modulation ratio is too large, the duty cycle of output is approximate to 1, thus losing the function of PWM control. If modulation ratio is too small, and duty ratio is too small, the control effect is not good. Therefore, it is necessary to perform PI control on the torque deviation signal, so that the modulation ratio is reasonably distributed between 0 and 1.

Imagine that when rotor is in the rising region of inductance or in the region near the minimum or maximum inductance, the voltage with the same duty cycle is applied, the torque variation is obviously different at the fixed switching frequency, which is not conducive to the suppression of torque ripple. Therefore, it is necessary to adjusting coefficients of duty cycle in different sectors. For regions where the torque changes rapidly, appropriately reduce the proportional parameter of PI control, so as to reduce the amplitude of torque change in each switch cycle. For regions where the torque changes slowly, proportional parameters of PI control can be appropriately increased to speed up torque response.

V. THE SIMULATION ANALYSIS

In order to verify the feasibility of the proposed DITC, a three-phase 12/8 SRM control system was simulated and analyzed in Matlab/Simulink environment. Simulation parameters are shown in the following table. Compare torque ripple suppression effect between the traditional DITC and the proposed DITC, and analyze the motor efficiency under the two control methods.

TABLE 1. Simulation parameters.

Parameters	Values
motor type	12/8 SRM
phase resistance	0.0026 Ω
maximum inductance	3.6 mH
minimum inductance	6 μH
moment of inertia	0.0526 kg·m^2
rate voltage	270 V
rate speed	13.5 kr/min
rate power	120 kW

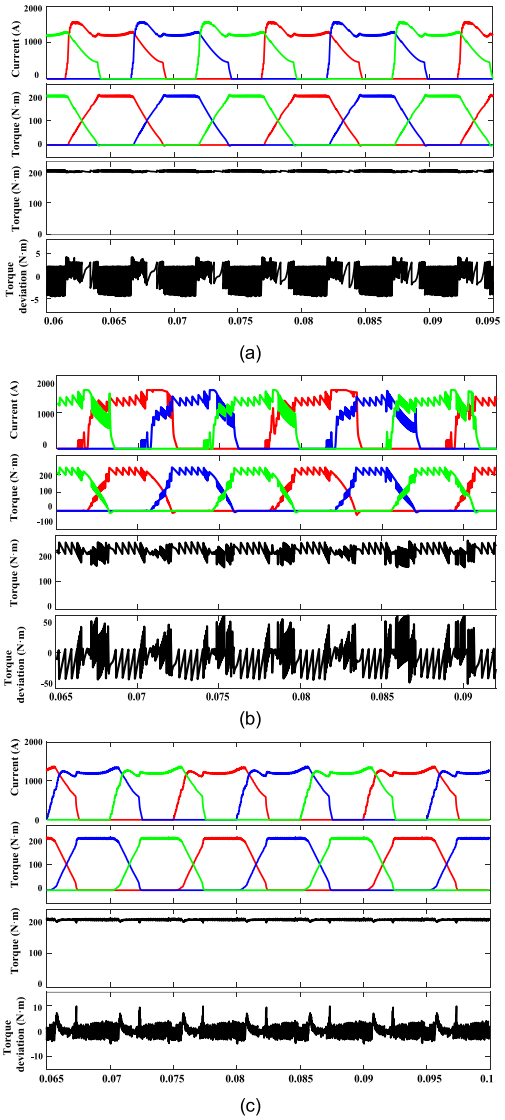

FIGURE 10. Simulation waveform at 500 r/min. (a) Traditional DITC I. (b) Traditional DITC II. (c) The proposed DITC.

Torque ripple ratio is defined as:

$$T_{\text{rip}} = \frac{T_{\text{e max}} - T_{\text{e min}}}{T_{\text{eva}}} \times 100\% \tag{4}$$

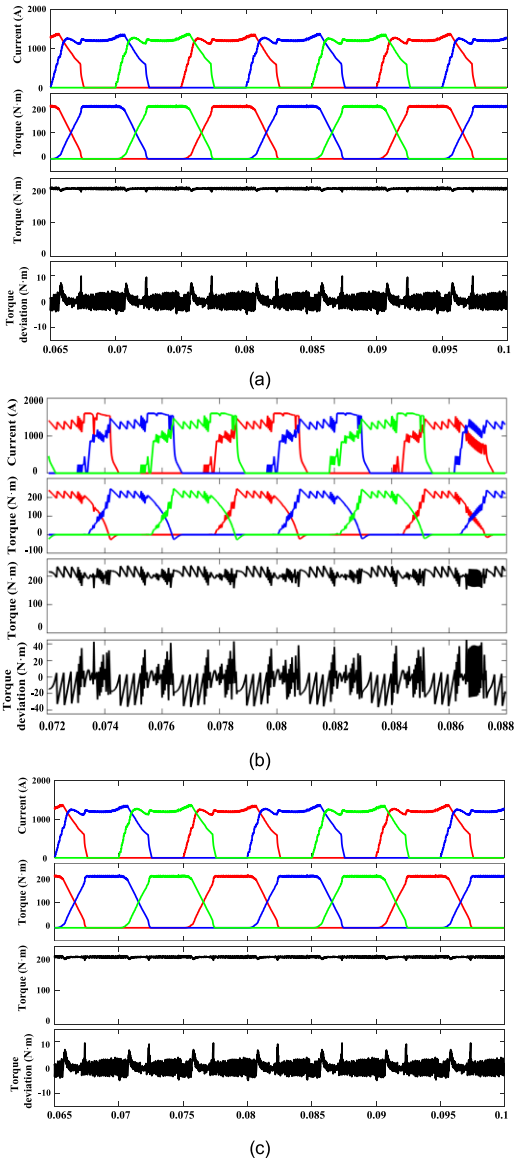

FIGURE 11. Simulation waveform at 1000 r/min. (a) Traditional DITC I. (b) Traditional DITC II. (c) The proposed DITC.

where, $T_{\text{rip}}$is torque ripple ratio, T_{emax}, T_{eva}, T_{emin} represent the maximum, minimum and average value of torque respectively.

A. TORQUE RIPPLE

For better explanation, traditional DITC I represents traditional DITC with variable switching frequency, which up to 500 kHz. Traditional DITC II represents traditional DITC with fixed switching frequency $f_{\text{k}} = 20$ kHz.

The simulation results under each operating condition showed below, from top to bottom, there are three phase current waveform, three phase torque waveform, total electromagnetic torque waveform and torque deviation waveform.

At a speed of 500 r/min, simulation results of three control methods are shown in figure 10. According to the calculation, the torque ripple ratios of traditional DITC I, traditional DITC

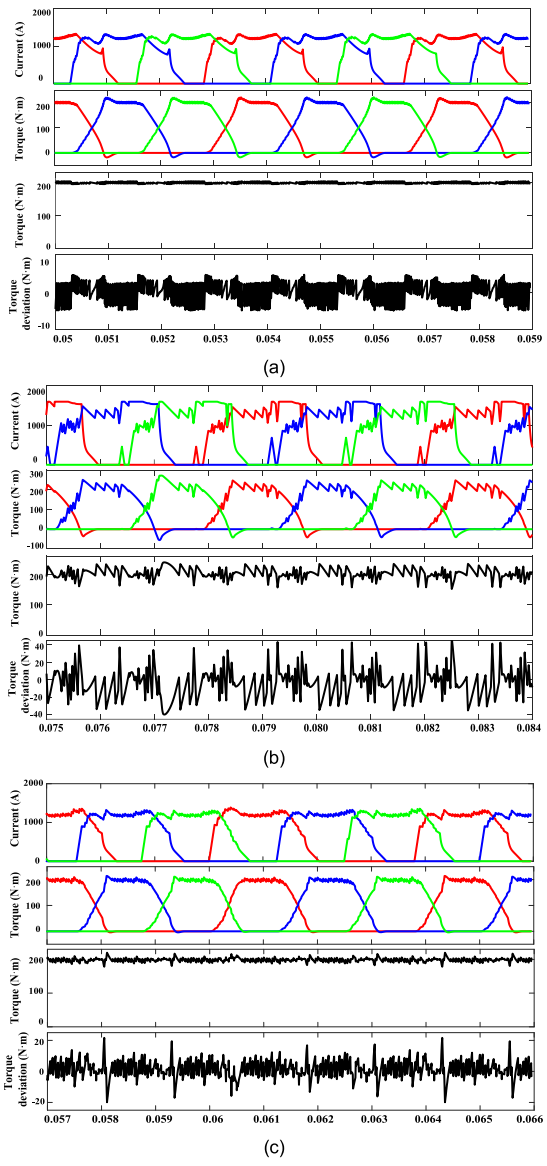

FIGURE 12. Simulation waveform at 2000 r/min. (a) Traditional DITC I. (b) Traditional DITC II. (c) The proposed DITC.

II, the proposed DITC are 4.2%, 44.85%, 7.27% respectively. It can be seen that traditional DITC I has very good torque ripple suppression under ideal conditions, but switching frequency is up to 500 kHz. Since the device has not reached such high switching frequency, such a good effect can't be achieved in the experiment. Under the control of fixed switching frequency of 20 kHz, it can be seen that torque ripple of the proposed DITC is much smaller than that of traditional DITC II.

Similarly, the simulation was conducted at a speed of 1000 r/min, and the simulation waveforms are shown in figure 11. It can be seen that torque ripple ratios of traditional DITC I, traditional DITC II, and the proposed DITC are 4.35%, 45%, 8.05% respectively.

The simulation waveforms under 2000 r/min are shown in figure 12. It can be obtained that the torque ripple ratios of traditional DITC I, traditional DITC II, the proposed DITC are 4.69%, 48.81%, 20.01% respectively.

TABLE 2. Comparison of torque ripples among traditional DITC I, traditional DITC II and the proposed DITC at different speeds.

Load torque (N·m)	Speed (r/min)	Method	T_{rip}
200	500	Traditional DITC I	4.2%
		Traditional DITC II	44.85%
		The proposed DITC	7.27%
	1000	Traditional DITC I	4.35%
		Traditional DITC II	45%
		The proposed DITC	8.05%
	2000	Traditional DITC I	4.69%
		Traditional DITC II	48.81%
		The proposed DITC	20.01%

TABLE 3. Comparison of currents of traditional DITC I and the proposed DITC at different speeds.

Load torque (N·m)	Speed (r/min)	Method	I_{max}(A)	I_{rms} (A)
200	500	Traditional DITC I	1568	812.2
		The proposed DITC	1358	768.3
	1000	Traditional DITC I	1357	789.3
		The proposed DITC	1342	776.3
	2000	Traditional DITC I	1326	792.6
		The proposed DITC	1324	768.5

Table 2 lists the torque ripple of three control modes at different speed. With the increase of the speed, the electromagnetic torque ripple also increases. At the same switching frequency, the torque ripple ratio of the proposed DITC is still half that of the traditional DITC II.

B. THE EFFICIENCY

In the case of the same load, the smaller current RMS is in one cycle, the higher the efficiency of the motor is. Table 3 lists the current indexes of the two control methods at different speeds.

Under the same working condition, the current RMS of the proposed DITC are all smaller than the traditional DITC I, indicating that the proposed DITC runs more efficiently. Comparing the maximum value of the current within a cycle between two methods, it can be seen that the proposed DITC can effectively control the current, and ensure that motor operate safely and reliably within the allowed current range.

VI. CONCLUSION

A novel DITC with fixed switching frequency is proposed to solve the problem of shaft breaking in the starting and generating system of SRM. The sector of the rotor is reclassified according to the curve of combined torque. According to the rotor sector, polarity of PWM output signal and duty cycle coefficient are determined; so as to acquire the control signal

considering both torque deviation and torque characteristics. The simulation results show that the proposed DITC achieves the very good torque ripple suppression effect under the finite switching frequency, and improves the motor operation efficiency, which is of great engineering practical value for aerospace starting and generating systems.

REFERENCES

[1] M. Krishnamurthy, C. S. Edrington, A. Emadi, P. Asadi, M. Ehsani, and B. Fahimi, "Making the case for applications of switched reluctance motor technology in automotive products," *IEEE Trans. Power Electron.*, vol. 21, no. 3, pp. 659–675, May 2006.

[2] S. Li, S. Zhang, T. G. Habetler, and R. G. Harley, "Modeling, design optimization, and applications of switched reluctance Machines—A review," *IEEE Trans. Ind. Appl.*, vol. 55, no. 3, pp. 2660–2681, Jun. 2019.

[3] G. Han, H. Chen, and G. Guan, "Low-cost SRM drive system with reduced current sensors and position sensors," *IET Electr. Power Appl.*, vol. 13, no. 7, pp. 853–862, Jul. 2019.

[4] L. Xu, D.-A. Zhao, C. Zhang, and R.-P. Ge, "Research on fault analysis and fault-tolerant control of valve electric actuator system based on SRM," in *Proc. 5th Int. Symp. Comput. Intell. Design*, Hangzhou, China, Oct. 2012, pp. 389–393.

[5] Y. Sozer, I. Husain, and D. A. Torrey, "Guidance in selecting advanced control techniques for switched reluctance machine drives in emerging applications," *IEEE Trans. Ind. Appl.*, vol. 51, no. 6, pp. 4505–4514, Nov. 2015.

[6] H. Chen and J. J. Gu, "Implementation of the three-phase switched reluctance machine system for motors and generators," *IEEE/ASME Trans. Mechatronics*, vol. 15, no. 3, pp. 421–432, Jun. 2010.

[7] S. Mendez, A. Martinez, W. Millan, C. E. Montano, and F. Perez-Cebolla, "Design, characterization, and validation of a 1-kW AC self-excited switched reluctance generator," *IEEE Trans. Ind. Electron.*, vol. 61, no. 2, pp. 846–855, Feb. 2014.

[8] C.-Y. Ho, J.-C. Wang, K.-W. Hu, and C.-M. Liaw, "Development and operation control of a switched-reluctance motor driven flywheel," *IEEE Trans. Power Electron.*, vol. 34, no. 1, pp. 526–537, Jan. 2019.

[9] E. Zhao, S. Song, Z. Ma, X. Zhang, L. Ning, and Y. Liu, "Design and initial testing of an integrated switched reluctance starter/generator system for unmanned aerial vehicle," *IEEE Trans. Power Electron.*, vol. 2, no. 4, pp. 377–383, Dec. 2018.

[10] D.-H. Lee, T. H. Pham, and J.-W. Ahn, "Design and operation characteristics of four-two pole high-speed SRM for torque ripple reduction," *IEEE Trans. Ind. Electron.*, vol. 60, no. 9, pp. 3637–3643, Sep. 2013.

[11] X. Deng, B. Mecrow, H. Wu, and R. Martin, "Design and development of low torque ripple variable-speed drive system with six-phase switched reluctance motors," *IEEE Trans. Energy Convers.*, vol. 33, no. 1, pp. 420–429, Mar. 2018.

[12] R. Madhavan and B. G. Fernandes, "Performance improvement in the axial flux-segmented rotor-switched reluctance motor," *IEEE Trans. Energy Convers.*, vol. 29, no. 3, pp. 641–651, Sep. 2014.

[13] S. Wang, "Research on switched reluctance motor control system for hybrid electric vehicle," Ph.D. dissertation, Huazhong Univ. Sci. Technol., Wuhan, China, 2005.

[14] C. Liu, Z. Deng, L. Xie, and K. Li, "The design of the simple structure-specified controller of magnetic bearings for the high-speed SRM," *IEEE/ASME Trans. Mechatronics*, vol. 20, no. 4, pp. 1798–1808, Aug. 2015.

[15] C. Ma and L. Qu, "Multiobjective optimization of switched reluctance motors based on design of experiments and particle swarm optimization," *IEEE Trans. Energy Convers.*, vol. 30, no. 3, pp. 1144–1153, Sep. 2015.

[16] S. R. Mousavi-Aghdam, M. R. Feyzi, N. Bianchi, and M. Morandin, "Design and analysis of a novel high-torque stator-segmented SRM," *IEEE Trans. Ind. Electron.*, vol. 63, no. 3, pp. 1458–1466, Mar. 2016.

[17] S. K. Sahoo, S. Dasgupta, S. K. Panda, and J.-X. Xu, "A Lyapunov function-based robust direct torque controller for a switched reluctance motor drive system," *IEEE Trans. Power Electron.*, vol. 27, no. 2, pp. 555–564, Feb. 2012.

[18] X. Ai-de, Z. Xianchao, H. Kunlun, and C. Yuzhao, "Torque-ripple reduction of SRM using optimised voltage vector in DTC," *IET Electr. Syst. Transp.*, vol. 8, no. 1, pp. 35–43, Mar. 2018.

[19] N. Yan, X. Cao, and Z. Deng, "Direct torque control for switched reluctance motor to obtain high Torque–Ampere ratio," *IEEE Trans. Ind. Electron.*, vol. 66, no. 7, pp. 5144–5152, Jul. 2019.

[20] N. H. Fuengwarodsakul, M. Menne, R. B. Inderka, and R. W. Dedoncker, "High-dynamic four-quadrant switched reluctance drive based on DITC," *IEEE Trans. Ind. Appl.*, vol. 41, no. 5, pp. 1232–1242, Sep. 2005.

[21] S. Yao and W. Zhang, "A simple strategy for parameters identification of SRM direct instantaneous torque control," *IEEE Trans. Power Electron.*, vol. 33, no. 4, pp. 3622–3630, Apr. 2018.

[22] C. Gan, J. Wu, Q. Sun, S. Yang, Y. Hu, and L. Jin, "Low-cost direct instantaneous torque control for switched reluctance motors with bus current detection under soft-chopping mode," *IET Power Electron.*, vol. 9, no. 3, pp. 482–490, Mar. 2016.

[23] J. Liang, D.-H. Lee, and J.-W. Ahn, "Direct instantaneous torque control of switched reluctance machines using 4-level converters," *IET Electr. Power Appl.*, vol. 3, no. 4, pp. 313–323, 2009.

[24] J. Ye, B. Bilgin, and A. Emadi, "An offline torque sharing function for torque ripple reduction in switched reluctance motor drives," *IEEE Trans. Energy Convers.*, vol. 30, no. 2, pp. 726–735, Jun. 2015.

[25] H. Li, B. Bilgin, and A. Emadi, "An improved torque sharing function for torque ripple reduction in switched reluctance machines," *IEEE Trans. Power Electron.*, vol. 34, no. 2, pp. 1635–1644, Feb. 2019.

[26] W. Peng, J. Gyselinck, J.-W. Ahn, and D.-H. Lee, "Torque sharing function control of switched reluctance machines with reduced current sensors," *China Electrotech. Soc. Trans. Electr. Mach. Syst.*, vol. 2, no. 4, pp. 355–362, Jan. 2019.

[27] A. Xu, C. Shang, J. Chen, J. Zhu, and L. Han, "A new control method based on DTC and MPC to reduce torque ripple in SRM," *IEEE Access*, vol. 7, pp. 68584–68593, 2019.

[28] X. Li and P. Shamsi, "Model predictive current control of switched reluctance motors with inductance auto-calibration," *IEEE Trans. Ind. Electron.*, vol. 63, no. 6, pp. 3934–3941, Jun. 2016.

[29] K. M. Rahman, S. Gopalakrishnan, B. Fahimi, A. V. Rajarathnam, and M. Ehsani, "Optimized torque control of switched reluctance motor at all operational regimes using neural network," *IEEE Trans. Ind. Appl.*, vol. 37, no. 3, pp. 904–913, May 2001.

[30] J. Wang, "Speed-assigned position tracking control of SRM with adaptive backstepping control," *IEEE/CAA J. Automatica Sinica*, vol. 5, no. 6, pp. 1128–1135, Nov. 2018.

SHUANGHONG WANG received the B.S. and Ph.D. degrees from Huazhong University Science and Technology, Wuhan, China, in 1998 and 2005, respectively.

He is currently an Associate Professor with the School of Electrical and Electronic Engineering, Huazhong University of Science and Technology. His research interests include power electronics and electric drive, and motor control for electric vehicles.

ZIHUI HU received the B.S. degree in electrical engineering and automation from Anhui University and Technology, Hefei, China, in 2018. She is currently pursuing the M.S. degree with the School of Electrical and Electronic Engineering, Huazhong University Science and Technology, Wuhan, China.

Her main research directions are torque ripple suppression and sensorless control of switched reluctance motors.

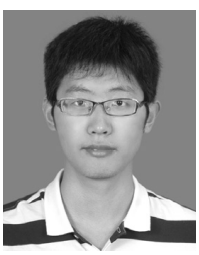

XIUPENG CUI (Member, IEEE) received the B.S. degree in applied physics from Shenyang University and Technology, Shenyang, China, in 2014. He is currently pursuing the Ph.D. degree with the School of Electrical and Electronic Engineering, Huazhong University Science and Technology, Wuhan, China.

His research interests include switched reluctance motor design and control, particularly for the optimization of low motor torque ripple, high efficiency synchronous reluctance motor design and control.